Smart Mater. Struct. **18** (2009) 024005 (5pp) doi:10.1088/0964-1726/18/2/024005

The dependence of infiltration pressure and volume in zeolite Y on potassium chloride concentration

Aijie Han[1], Weiyi Lu[2], Taewan Kim[3], Venkata K Punyamurtula[2] and Yu Qiao[2,3,4]

[1] Department of Chemistry, University of Texas—Pan America, Edinburg, TX 78539, USA
[2] Department of Structural Engineering, University of California—San Diego, La Jolla, CA 92093-0085, USA
[3] Program of Materials Science and Engineering, University of California—San Diego, La Jolla, CA 92093-0085, USA

E-mail: yqiao@ucsd.edu

Received 7 October 2008
Published 20 January 2009
Online at stacks.iop.org/SMS/18/024005

Abstract
In a previous work we developed a volume-memory liquid that can expand or shrink significantly as the temperature varies. The working mechanism is based on the thermally induced infiltration and defiltration of an electrolyte solution in the nanopores. In the current study, we investigate the influence of electrolyte concentration on the infiltration behavior, as well as its dependence on temperature. The testing data show that, as the electrolyte concentration varies, the effective interfacial tension changes rapidly. This phenomenon can be attributed to the amplification effect of nanopore surfaces on the solid–liquid interaction. It provides a scientific basis for developing smart liquids for various temperature and pressure ranges.

(Some figures in this article are in colour only in the electronic version)

1. Introduction

Developing high-performance smart materials has been a continuous effort since the discovery of the shape-memory characteristic of titanium–nickel alloy (Trochu *et al* 1999). Shape-memory alloys and polymers are activated via phase transformations (Gandhi and Thompson 1992). As the temperature changes, their atomic or molecular configurations can vary accordingly, accompanied by significant volume increase or decrease. As a result, at the macroscopic scale the material shape can be thermally controlled. Conventional smart materials are solids. As the phase transformation is induced repeatedly and the local volume change occurs, fatigue damage and/or fracture may considerably limit the system reliability (Chopra 2002, Kuna 2006). Moreover, the energy density of these materials is still quite low (Otsuka and Wayman 1999). To solve these problems, new mechanisms need to be investigated.

In a recent study, we developed a novel smart material—nanoporous material functionalized (NMF) liquid (Han and Qiao 2007a). It is a milk-like liquid suspension that can expand or shrink significantly as the temperature is adjusted. The working mechanism is based on the well-known thermocapillary effect (Sefiane and Ward 2007); i.e. the solid/liquid surface tension and the solid–liquid interfacial tension are dependent on the temperature. With appropriate surface treatment, a solid surface can be wettable to a liquid in a certain temperature range and nonwettable once the temperature is beyond this range (Qiao *et al* 2007b, Han and Qiao 2007b, 2007c). If this phenomenon is applied to a nanoporous material, it can lead to temperature-controlled liquid infiltration and defiltration. As depicted in figure 1, an NMF liquid is produced by dispersing nanoporous particles in a liquid phase. The particle size is typically 1–100 μm and the nanopore size is usually 1–10 nm. In figure 1(a), the nanopore inner surfaces are wettable to the liquid, and therefore the nanoporous particles are soaked up. The total system volume can be assessed as $V_0 = V_l + V_s - V_p$,

[4] Author to whom any correspondence should be addressed.

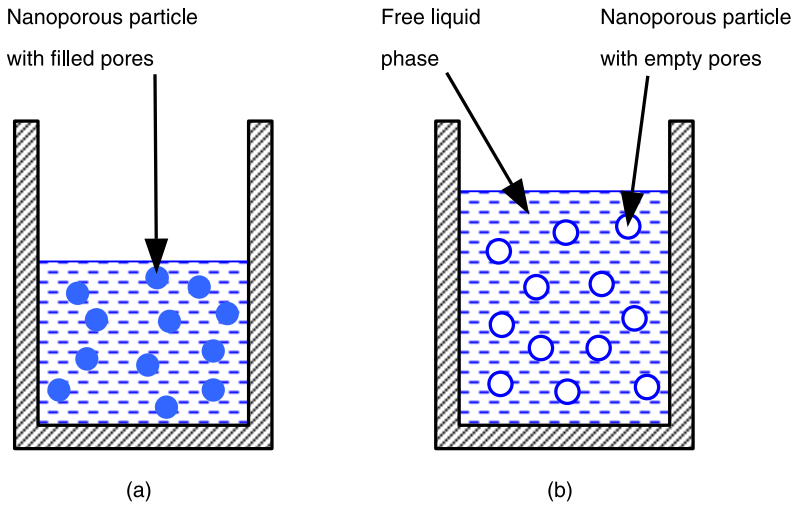

Figure 1. Schematic diagrams of the volume-memory liquid: (a) filled nanoporous particles and (b) empty nanoporous particles.

with V_l, V_s, and V_p being the volumes of liquid, solid, and nanopores, respectively. When the temperature changes, due to the difference in changing rates of the surface tensions of the liquid and solid phases, the interfacial tension, $\Delta\gamma$, may either increase or decrease (Erbil 2006), causing the variation in wettability. Figure 1(b) shows that when $\Delta\gamma$ becomes positive, i.e. when the nanopore surfaces are effectively nonwettable, the confined liquid can defiltrate out of the nanopores, and thus the system volume expands. The expanded system volume can be estimated as $V_e = V_l + V_s$. The deformability can be calculated as $\xi = V_p/(V_l + V_s)$, which is typically 10–20% for zeolite Y based systems. Due to the small length scale involved in the liquid motion in the nanoenvironment, the nature of liquid–solid interaction is quite different from that at large scale (Qiao *et al* 2007a), and the infiltration/defiltration can be regarded as an effective phase transformation process (Han *et al* 2006), since the confined liquid phase and the free liquid phase are stable at different temperatures. The energy density of the smart liquid can be taken as $E = \Delta\gamma A$, where $A \approx 10^2$–10^3 m^2 g^{-1} is the specific surface area. Due to the large value of A, for solid–liquid systems with $\Delta\gamma$ around 10 mJ m^{-2} (Han and Qiao 2007b, 2007c), E can be 1–10 J g^{-1}, which is two orders of magnitude higher than the value of 50 mJ g^{-1} reported for Ti–Ni alloys (Wei *et al* 1998).

In a previous experiment on smart liquid (Han and Qiao 2007a), zeolite Y that had a well crystallized porous structure was employed as the nanoporous phase (Baerlocher *et al* 2007). It was noticed that the liquid infiltration and defiltration behavior was dependent on the liquid composition. For instance, in a pure water based system, no volume-memory behavior could be observed even when the temperature was adjusted in a broad range. The liquid phase should be modified by an electrolyte, after which the wetting-to-dewetting transition could be triggered by a relatively small temperature variation of only a few degrees celsius. Since the liquid motion in the nanopores is the key factor dominating the smart liquid properties, the influence of the electrolyte concentration and the temperature on the infiltration pressure will be investigated in the current study.

2. Experimental details

The framework type of zeolite Y is FAU, which has a 12-ring channel viewed along [111], with the nominal size of 0.74 nm × 0.74 nm; its atomic structure was described in detail by Auerbach *et al* (2003). The material was analyzed by using a Micromeritics TriStar 3000 gas adsorption analyzer. The effective nanopore size was determined as 0.6 nm, and the specific surface area was 710 m^2 g^{-1} (Han and Qiao 2007a). The specific nanopore volume was 220 mm^3 g^{-1}. The initial silica/alumina ratio was 80. The material was heated at 120 °C for 3 h so that it was dehydrated. It was then treated in saturated silicon tetrachloride vapor in nitrogen at 400 °C for 0.5 h, followed by thorough rinsing with distilled water and calcination at 500 °C for 1 h. The aluminum content was further decreased by hydrothermally treating the sample at 650 °C for 72 h. Finally, the material was washed repeatedly in warm water and dried in vacuum.

About 1 g of the zeolite sample was suspended in 4 g of aqueous solution of potassium chloride (KCl). The KCl concentration, [KCl], ranged from 18% to 24%. The suspension was sealed in a poly(methyl methacrylate) cylinder. By intruding a stainless steel piston into the cylinder, an external pressure, P, was applied on the liquid suspension. The piston motion was controlled by a type 5582 Instron machine in displacement-control mode at the rate of 1 mm min^{-1}. The cross-sectional area of the piston, A_p, was 286 mm^2. When the applied load reached about 14.8 kN, the piston was moved back at the same speed. The variation in specific volume of the zeolite suspension, ΔV, was calculated as dA_p/m, with d being the piston displacement and m the mass of zeolite crystals. At a low pressure level, the slope of the sorption curve was relatively large. When the infiltration happened, the slope of the sorption curve became smaller. When the infiltration finished, the slope of the sorption curve became large again. To investigate the thermally controlled liquid motion, the infiltration experiments were performed with 18%, 20%, 22%, and 24% KCl solution at various temperatures in the range 20–80 °C. For each system, at least three samples

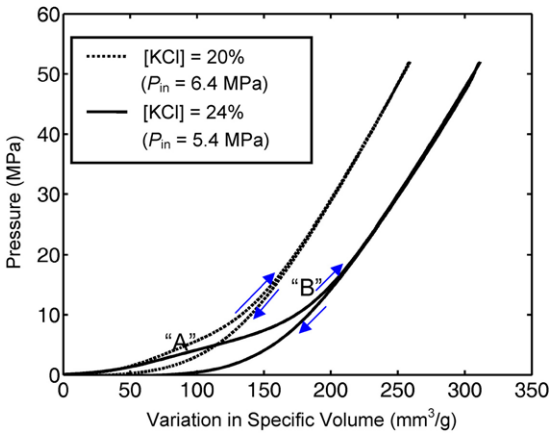

Figure 2. Typical sorption curves at 20 °C.

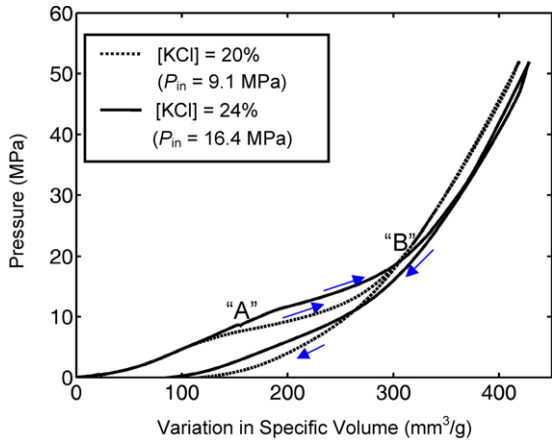

Figure 3. Typical sorption curves at 80 °C.

were tested. It took about 0.9 min to complete a loading process and about the same time for an unloading process. The temperature was maintained by a water bath. Figures 2 and 3 show typical sorption curves at room temperature and at elevated temperature, respectively. The infiltration plateau is shown as 'AB', as will be discussed below.

3. Results and discussion

Usually, if the silica/alumina ratio is higher than 18, a zeolite can be regarded as hydrophobic (Xu *et al* 2007), which is in agreement with the phenomenon observed in gas adsorption analysis that an external pressure must be applied to force water vapor into the nanopores (Yang 1997). However, the wettability of nanopore inner surfaces is quite different in liquid water. When the zeolite sample is immersed in pure water, the sample can be soaked up immediately. Under this condition, because the nanopores are filled, the response of the zeolite suspension to external pressure is quite linear; that is, $K = P/\Delta V$ is nearly constant, dominated by the bulk modulus of water. Even after the material is treated by silicon tetrachloride and water vapors, spontaneous infiltration can still take place under ambient pressure. Clearly, it is much easier for water molecules to enter the nanopores in the bulk phase than in the vapor phase, probably because in the confining nanoenvironment adjacent molecules can lead to the reduction in energy barrier between tetrahedral sites.

After the treatment, the effective degree of hydrophobicity of the zeolite has nearly been saturated. One way to further increase $\Delta\gamma$ is to modify the liquid composition to adjust the smart liquid properties. When [KCl] is relatively low, the zeolite sample is still wettable to the liquid phase. When [KCl] is lower than 20%, no infiltration plateau can be observed in the sorption isotherm curve. As shown in figure 2, when [KCl] is 20%, pressure induced infiltration takes place. Shortly after the pressure increase, an infiltration plateau is formed, demonstrating the characteristics of a smart liquid. In the infiltration plateau, the system volume decreases rapidly with a small pressure increment, indicating that the dominant deformation mechanism is no longer the linear compression of free liquid phase. That is, as the pressure increases, the barrier effect of the nanopore surfaces can be overcome. Once the accessible nanopores are filled, the system deformability significantly decreases, and the slope of the sorption curve increases significantly. The infiltration pressure is close to that of 24% [KCl]. As [KCl] = 20%, the infiltration volume, i.e. the width of the infiltration plateau, is only about 60 mm^3 g^{-1}, 1/4 of the total nanopore volume, suggesting that most of the nanopore surfaces have been wetted before the pressure is applied. In the following discussion, for self-comparison purposes, the infiltration plateau is defined as the part of the sorption isotherm between the two points where the local slopes equal 50% of that of the high pressure stage. The portion of the nanopores that are filled spontaneously is probably close to the open ends, the details of which are still under investigation.

As [KCl] increases, the effective degree of hydrophobicity of the material keeps increasing. When [KCl] = 24%, the infiltration plateau ('AB' in figure 2) becomes much clearer. The infiltration consists of two stages. At a low pressure level, the slope of the sorption curve is relatively large. At a higher pressure level, a smaller pressure increment is needed to reduce the system volume, which may be associated with the promotion effect of the confined liquid. The specific infiltration volume is around 100 mm^3 g^{-1}, still smaller than the nanopore volume measured by the gas adsorption technique but much larger than that of the 20% KCl solution. Clearly, as [KCl] increases, the nanopore surfaces are more nonwettable, and therefore little nanoporous space can be filled under ambient pressure. Only when an external pressure is applied can the liquid infiltration take place. The difference between the pore volumes in liquid infiltration and gas adsorption may be related to the van der Waals distance between the confined liquid molecules and the nanopore walls.

When the temperature increases, the degree of hydrophobicity of the zeolite becomes considerably higher, as shown in figure 3. At 80 °C, even in 20% KCl solution the infiltration profile is quite clear. The specific infiltration volume is about 100 mm^3 g^{-1}, close to that of 24% KCl at 20 °C, which represents the upper limit of nanoporous space. When the pressure is lower than 6 MPa, little evidence of infiltration can be observed. A regular infiltration plateau is formed in the pressure

range from 6 to 13 MPa. As the pressure further increases, the slope of the sorption curve converges to that of the free liquid phase. According to a Carnot cycle analysis, the net output energy is $\Delta\gamma A$ or $P_{\text{in}} V_{\text{in}}$, where P_{in} is the infiltration pressure and V_{in} is the infiltration volume. For the sake of simplicity, the infiltration pressure is taken as the pressure at the middle point of the infiltration plateau. If V_{in} is taken as 100 mm^3 g^{-1} and P_{in} is taken as 9 MPa, the specific energy density can be calculated as 0.9 J g^{-1}, much larger than that of Ti–Ni alloys (50 mJ g^{-1}). When [KCl] is changed to 24%, these characteristics remain the same, except that the infiltration pressure range increases by nearly 80%. If P_{in} is taken as 16.4 MPa, the specific energy density can be calculated as 1.6 J g^{-1}, much larger than that of 22% KCl at 80 °C. It is clear that the degree of hydrophobicity is increased with temperature. Moreover, the infiltration and defiltration process is quite reversible, suitable for applications of smart liquids.

Figure 4 shows the infiltration pressure as a function of the potassium chloride concentration and the temperature. In general, P_{in} increases with [KCl], as discussed above. At 20 °C, when the electrolyte concentration is relatively low, the pressure induced infiltration cannot occur fully. Since only the nanopores of high infiltration resistance are involved, the average value of P_{in} is higher than that at larger [KCl]. Note that this is caused by the limitation of the definition of infiltration pressure used in the current study, and may not reflect the variation in degree of hydrophobicity. At an elevated temperature, since the sorption curve reflects the behavior of all the accessible nanopores, the curves are more regular. According to the classic Laplace–Young equation (Shikhmurzaev 2007), the effective solid–liquid interfacial tension can be estimated as $\Delta\gamma = P_{\text{in}} r/2$, with $r = 0.3$ nm being the effective nanopore radius. At 40 °C, when [KCl] increases from 18% to 24%, $\Delta\gamma$ changes quite linearly from 0.9 to 1.8 mJ m^{-2} by nearly 100%; that is, the effective interfacial tension in the nanopores is very sensitive to the electrolyte concentration. The electrolyte concentration effect is even more pronounced when the temperature is changed to 80 °C, where, as [KCl] varies in the same range, $\Delta\gamma$ increases from 1.1 to 2.5 mJ m^{-2} by about 130%. That is, as the temperature increases, the hydrophobicity increases more pronouncedly. At all temperatures, the reversibility of the NMF liquid is superior. The infiltration/defiltration curves can be repeated more than ten times without detectable system degradation.

At a large solid surface, while the solid–liquid interfacial tension is dependent on the liquid composition, the variation in $\Delta\gamma$ is typically only 20–30% between pure water and saturated solutions (Riviere and Myhra 1998). In the nanopores, however, $\Delta\gamma$ changes by more than 100% when the potassium chloride concentration varies by only 6%. This may be attributed to the confinement effect of the nanopore walls. At a large surface, the solvated cations distribute in the outer Helmholtz plane (OHP), which is a few angstroms from the solid phase (Schmickler 1996, Hartland 2004). The interfacial tension is determined by the interaction between the solid atoms and the solvated ions, as well as the water molecules. In a nanopore, especially when the nanopore size

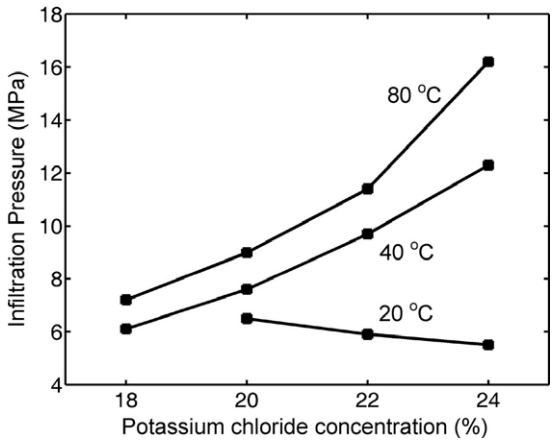

Figure 4. The infiltration pressure as a function of the potassium chloride concentration. The data point for 18% solution at 20 °C is not shown since no infiltration can be measured under this condition.

is comparable with the OHP distance, a regular layered ion structure cannot be formed. The solvated ions are surrounded by solid atoms from all directions, and therefore the effect caused by the increase in ion concentration, for instance the variation in interfacial tension and the infiltration pressure, can be amplified. Since the nanoporous structure is stable in the temperature range under investigation, a similar electrolyte concentration effect can be observed at all testing temperatures. Such a phenomenon can be used for adjusting the working temperature range and/or the pre-loading range of smart liquids, depending on the functional requirements of energy density, working conditions, etc.

4. Concluding remarks

The current study is focused on an experimental investigation of the infiltration behavior of electrolyte solutions in zeolite Y. While the details of the liquid motion in nanopores are still under investigation, it is noticed that the effective solid–liquid interfacial tension in nanopores is highly sensitive to the electrolyte concentration, which may be related to the unique confinement environment in nanoporous material. As a result, with the addition of potassium chloride, both the infiltration pressure and the infiltration volume tend to increase. This finding provides a scientific basis for adjusting the ranges of temperature and pressure of nanoporous material functionalized liquids.

Acknowledgments

This study was supported by The National Science Foundation and The Sandia National Lab under Grant No. CMS-0623973.

References

Auerbach S M, Carrado K A and Dutta P K 2003 *Handbook of Zeolite Science and Technology* (New York: Dekker)

Baerlocher Ch, McCusker L B and Olson D H 2007 *Atlas of Zeolite Framework Types* (Oxford: Elsevier)

Chopra I 2002 Review of state of art of smart structures and integrated systems *AIAA J.* **40** 2145–87

Erbil H Y 2006 *Surface Chemistry of Solid and Liquid Interfaces* (Oxford: Wiley–Blackwell)
Gandhi M V and Thompson B D 1992 *Smart Materials and Structures* (New York: Springer)
Han A, Kong X and Qiao Y 2006 Pressure induced infiltration in nanopores *J. Appl. Phys.* **100** 014308
Han A and Qiao Y 2007a A volume memory liquid *Appl. Phys. Lett.* **91** 173123
Han A and Qiao Y 2007b Thermal effects on infiltration of a solubility sensitive volume memory liquid *Phil. Mag. Lett.* **87** 25–31
Han A and Qiao Y 2007c Infiltration pressure of a nanoporous liquid spring modified by an electrolyte *J. Mater. Res.* **22** 644–8
Hartland S 2004 *Surface and Interfacial Tension: Measurement, Theory, and Applications* (New York: Dekker)
Kuna M 2006 Finite element analyses of cracks in piezoelectric structures: a survey *Arch. Appl. Mech.* **76** 725–45
Qiao Y, Cao G and Chen X 2007a Effects of gas molecules on nanofluidic behaviors *J. Am. Chem. Soc.* **129** 2355–9
Qiao Y, Punyamurtula V K, Han A, Kong X and Surani F B 2007b Temperature dependence of working pressure of a nanoporous liquid spring *Appl. Phys. Lett.* **89** 251905
Otsuka K and Wayman C M 1999 *Shape Memory Materials* (Cambridge: Cambridge University Press)
Riviere J C and Myhra S 1998 *Handbook of Surface and Interface Analysis* (New York: Dekker)
Schmickler W 1996 *Interfacial Electrochemistry* (Oxford: Oxford University Press)
Sefiane K and Ward C A 2007 Recent advances on thermocapillary flows and interfacial conditions during the evaporation of liquids *Adv. Colloid Interface Sci.* **134/135** 201–23
Shikhmurzaev Y D 2007 *Capillary Flows with Forming Interfaces* (Boca Raton, FL: CRC Press)
Trochu F, Brailovski V and Galibois A 1999 *Shape Memory Alloys: Fundamentals, Modeling and Industrial Applications* (Warrendale, PA: TMS)
Wei Z G, Sandstrom R and Miyazaki S 1998 Shape memory materials and hybrid composites for smart systems—part I. Shape memory materials *J. Mater. Sci.* **33** 3743–62
Xu R, Pang W, Yu J, Huo Q and Chen J 2007 *Chemistry of Zeolites and Related Porous Materials* (New York: Wiley)
Yang R T 1997 *Gas Separation and Adsorption Processes* (London: Imperial College Press)